

## Magnetic Resonance and Electromagnetic Wave Propagation in Materials Having $g$ -Factor Anisotropies

George T. Rado

*Naval Research Laboratory, Washington, D.C. 20390*

(Received 7 September 1971)

A method is presented for deriving from an ionic spin Hamiltonian a classical equation of motion of the magnetization which remains valid for materials in which the  $g$  factor is anisotropic. The Hamiltonian invoked to illustrate the method includes the Zeeman term as well as terms corresponding to the local field, anisotropic exchange, and "one-ion" anisotropy. This new equation of motion is used first to calculate, in the magnetostatic limit, the small-signal complex susceptibility of the Ising-like antiferromagnet  $\text{DyPO}_4$  exposed to a saturating static magnetic field and then, in conjunction with Maxwell's equations, to treat the "dimensional resonances" arising from electromagnetic propagation effects. After introducing approximations appropriate to Ising-like systems, an explicit expression is obtained for the field-dependent transmission through a monocrystalline  $\text{DyPO}_4$  slab whose thickness is comparable to the wavelength. Propagation effects are shown to offer a possible explanation of the asymmetric line shape observed in a recent far-infrared laser resonance experiment on  $\text{DyPO}_4$  and to constitute a probably unique explanation of the experimental fact that the transmission at fields near resonance can exceed that at fields far from resonance. More generally, propagation effects are shown to be difficult to avoid at any wavelength in transversely excited, strongly Ising-like systems.

### I. INTRODUCTION

The high resolution obtained by the use of lasers in recent magnetic resonance experiments has made it possible to measure not only resonance frequencies but also linewidths and even line shapes at wavelengths in the far-infrared region of the spectrum.<sup>1-3</sup> It seems worth remarking, therefore, that the effects of electromagnetic propagation on the linewidths and line shapes should be considered because these effects may well cause the observed resonance lines to be distorted. The reason is that the wavelengths in the far infrared are so short that it is difficult to avoid propagation effects by preparing samples whose thickness is small compared to the wavelength  $\lambda$  inside the sample. In the far-infrared magnetic resonance experiments<sup>1-3</sup> the sample thickness (0.1–0.04 cm) is indeed comparable to the free-space wavelength  $\lambda_0$  (0.03–0.02 cm) and thus probably comparable to  $\lambda$ . In magnetic resonance experiments at microwave frequencies, on the other hand,  $\lambda_0$  is at least 50 times longer than in the far infrared so that propagation effects can usually be avoided by preparing samples whose linear dimensions are small compared to  $\lambda$ .

The crystals used in the magnetic resonance experiments, holmium ethyl sulfate<sup>1</sup> and dysprosium orthophosphate,<sup>2,3</sup> have a spectroscopic splitting factor  $g$  which is so strongly anisotropic that these crystals are "Ising-like" systems. We wish to remark, therefore, that attempts to avoid propagation effects in Ising-like systems by the use of sufficiently thin samples may not be successful even

if such samples can be fabricated. This possibility is due to the fact that the magnetic resonance experiments<sup>1-3</sup> necessarily involve excitations transverse to the Ising axis so that, as explained later on, the observed resonance absorption may be too weak at any wavelength to be observable with presently available apparatus.

The purpose of this paper<sup>4</sup> is to explore the quantitative consequences of the above-mentioned remarks by calculating magnetic resonance and electromagnetic propagation effects in materials having  $g$ -factor anisotropy. In Sec. II (which is supplemented by the Appendix), we present a method for deriving from an ionic spin Hamiltonian a classical equation of motion of the magnetization which differs from the familiar Landau-Lifshitz equation in that it remains valid for materials in which the  $g$  factor is anisotropic. Previous attempts to obtain such an equation of motion either included only the Zeeman term<sup>5</sup> of the total Hamiltonian (and involved a  $g$  tensor which was assumed to be symmetric) or consisted of postulating equations<sup>6</sup> fulfilling specified conservation requirements. We illustrate the method with a Hamiltonian containing the Zeeman term (involving a  $g$  tensor which need not be symmetric) as well as a local field term, an anisotropic exchange term (expressed in the molecular field approximation), and a "one-ion" anisotropy term. In Sec. III, we particularize the classical equation of motion derived on the basis of the three former terms and use it to calculate, in the magnetostatic limit, the resonance frequency and the small-signal complex susceptibility of the Ising-like antiferromagnet

DyPO<sub>4</sub> when it is exposed to a saturating static magnetic field. Also contained in this section is the introduction of approximations appropriate to Ising-like systems and a discussion of various effective fields in the magnetic resonance of materials having  $g$ -factor anisotropy. In Sec. IV, we solve the particularized equation of motion in conjunction with Maxwell's equations and treat the "dimensional resonances" arising from electromagnetic propagation effects. Thus we obtain an explicit expression for the magnetic-field-dependent transmission through a monocrystalline DyPO<sub>4</sub> slab whose thickness is comparable to  $\lambda$ . We find that propagation effects offer a possible explanation of the observed asymmetry<sup>2,3</sup> of the resonance and that they offer a probably unique explanation of the experimental fact<sup>2,3</sup> that the transmission at fields near resonance can exceed that at fields far from resonance.

Since the present work was motivated largely by the far-infrared DyPO<sub>4</sub> experiments,<sup>2,3</sup> it is unfortunate that the brittleness of the currently available DyPO<sub>4</sub> crystals prevents them from being polished sufficiently well to allow a more critical comparison between experiment and theory. It should be noted, therefore, that the applicability of our calculations is not confined to the "prototype" material DyPO<sub>4</sub> but extends to the analysis of magnetic resonance and electromagnetic propagation experiments in other materials which are highly anisotropic.

## II. EQUATION OF MOTION

### A. Zeeman Hamiltonian

We start with the equation of motion

$$\frac{i\hbar d}{dt} \langle \vec{\mu}_{sp} \rangle = \langle [\vec{\mu}_{sp}, \mathcal{H}] \rangle, \quad (1)$$

where  $\langle \rangle$  denotes the average value in a combined quantum mechanical and statistical sense. To each magnetic ion we assign the spin Hamiltonian  $\mathcal{H}$  and the spin magnetic moment

$$\vec{\mu}_{sp} = -2 |\mu_B| \vec{S}, \quad (2)$$

where  $\vec{S}$  is the ionic spin and  $\mu_B$  the (intrinsically negative) Bohr magneton. In the simplest situation we restrict  $\mathcal{H}$  to the Zeeman Hamiltonian

$$\mathcal{H}_Z = |\mu_B| \vec{S} \cdot \vec{g} \cdot \vec{H}, \quad (3)$$

where  $\vec{H}$  is the magnetic field and  $\vec{g}$  is the tensor representing the  $g$  factor. By combining Eqs. (1)–(3) with the commutation relations  $\vec{S} \times \vec{S} = i\vec{S}$ , we then obtain

$$\frac{\gamma_0^{-1} d}{dt} \langle \vec{\mu}_{sp} \rangle = \langle \vec{\mu}_{sp} \rangle \times (\frac{1}{2} \vec{g} \cdot \vec{H}), \quad (4)$$

where  $\gamma_0$  is defined by

$$\gamma_0 = -2 |\mu_B| / \hbar. \quad (5)$$

If we now introduce

$$\vec{M}_{sp} = N \langle \vec{\mu}_{sp} \rangle, \quad (6)$$

where  $N$  is the number of magnetic ions per unit volume, then Eq. (4) becomes

$$\frac{\gamma_0^{-1} d}{dt} \vec{M}_{sp} = \vec{M}_{sp} \times (\frac{1}{2} \vec{g} \cdot \vec{H}), \quad (7)$$

which is one form of the classical equation of motion for the situation  $\mathcal{H} = \mathcal{H}_Z$ . Equation (7) shows that in this situation the anisotropy of  $\vec{g}$  can be taken into account, at least for some purposes, by proceeding as if  $\gamma_0$  (which involves  $g=2$ ) were unchanged and the magnetic field had the value  $\frac{1}{2} \vec{g} \cdot \vec{H}$ . This result has long been known in antiferromagnetic resonance<sup>7</sup> and also in paramagnetic resonance.<sup>5</sup> What has not always been made clear, however, is that Eq. (7) contains the spin magnetization  $\vec{M}_{sp}$ , rather than the total magnetization  $\vec{M}$ . To replace  $\vec{M}_{sp}$  by  $\vec{M}$  in Eq. (7) is definitely incorrect because the anisotropy of  $\vec{g}$  means that  $\vec{M}_{sp}$  and  $\vec{M}$  are not parallel. In some special cases, of course, the calculated resonance frequency is unaffected by such a replacement. If  $\vec{H}$  is simply the externally applied field, for example, then the kinematical interpretation of Eq. (7) shows that the circular precession frequency  $-\frac{1}{2} \gamma_0 |\vec{g} \cdot \vec{H}|$  remains unaltered if  $\vec{M}_{sp}$  is replaced by  $\vec{M}$ . It may be noted parenthetically that this frequency is exactly the same as that obtained quantum mechanically for magnetic dipole transitions from Eqs. (3) and (5). However, calculations of resonance frequencies in more complicated cases (e.g., in the presence of demagnetizing effects) and calculations of susceptibilities in all cases do require that  $\vec{M}_{sp}$  and  $\vec{M}$  be distinguished carefully. We do this by noting that Eq. (3) may be rewritten in the form  $\mathcal{H}_Z = -\vec{\mu}_{sp} \cdot (\frac{1}{2} \vec{g} \cdot \vec{H})$ , which suggests Eq. (7), or in the form  $\mathcal{H}_Z = -\vec{\mu} \cdot \vec{H}$ , which contains

$$\vec{\mu} = -|\mu_B| \vec{S} \cdot \vec{g} = \vec{\mu}_{sp} \cdot \frac{1}{2} \vec{g}, \quad (8)$$

the total magnetic moment per ion. Combining  $\vec{M} = N \langle \vec{\mu} \rangle$  with Eqs. (6) and (8) gives  $\vec{M} = \vec{M}_{sp} \cdot \frac{1}{2} \vec{g}$ , so that we obtain

$$\vec{M}_{sp} = 2\vec{M} \cdot \vec{g}^{-1}, \quad (9)$$

provided we assume that  $\vec{g}^{-1}$  exists. Substitution of Eq. (9) into Eq. (7) yields

$$\frac{\gamma_0^{-1} d}{dt} (\vec{M} \cdot \vec{g}^{-1}) = (\vec{M} \cdot \vec{g}^{-1}) \times (\frac{1}{2} \vec{g} \cdot \vec{H}), \quad (10)$$

which is our desired equation of motion of  $\vec{M}$  for the situation  $\mathcal{H} = \mathcal{H}_Z$ . Unlike an earlier result due to Pryce,<sup>5</sup> Eq. (10) is independent of the coordinate system and remains valid if  $\vec{g}$  is not symmetric. The latter generalization is particularly useful because  $\vec{g}$  need not<sup>8</sup> be symmetric in all crystals.

### B. Other Hamiltonians

Turning now to more general situations, we first consider the class of Hamiltonians which can be written in the form

$$\mathcal{H}_{\text{eff}} = -\vec{\mu}_{\text{sp}} \cdot \vec{H}_{\text{eff}}, \quad (11)$$

where the effective field  $\vec{H}_{\text{eff}}$  is independent of  $\vec{S}$  but may depend on  $\langle \vec{S} \rangle$ . We substitute  $\mathcal{H} = \mathcal{H}_{\text{eff}}$  into Eq. (1) and proceed in a manner analogous to that used in deriving Eq. (10). The resulting equation of motion

$$\frac{\gamma_0^{-1} d(\vec{M} \cdot \vec{g}^{-1})}{dt} = (\vec{M} \cdot \vec{g}^{-1}) \times \vec{H}_{\text{eff}} \quad (12)$$

clearly contains Eq. (10) as that special case in which  $\vec{H}_{\text{eff}}$  is given by  $\frac{1}{2} \vec{g} \cdot \vec{H}$ . Also contained in Eq. (12) is that special case in which  $\vec{H}_{\text{eff}}$  denotes a (generally anisotropic or even antisymmetric) molecular field and/or its spatial derivatives. It should be noted that Eq. (12), as well as every other equation of this paper, does remain valid if  $\vec{S}$  represents the fictitious spin  $\frac{1}{2}$  of a Kramers doublet rather than some arbitrary true spin. The calculation presented in Sec. III is an example of the use of Eq. (12) in a situation involving not only  $\vec{H}$  but also an anisotropic molecular field in conjunction with such a fictitious spin.

Next we consider the class of Hamiltonians which cannot be written in the form of Eq. (11). One member of this class is the (generally anisotropic or even antisymmetric) exchange Hamiltonian in a situation in which the latter is *not* treated in the molecular field approximation. Such a situation will not be considered here. Other members of this class are the various Hamiltonians representing single-ion anisotropy energies. These are not relevant to the problem of Sec. III because in  $\text{DyPO}_4$  the fictitious spin is  $\frac{1}{2}$  so that the single-ion anisotropy energy vanishes. To avoid interrupting the continuity of the presentation, therefore, we relegate to the Appendix the derivation of the equation of motion for a situation in which the Hamiltonian represents single-ion anisotropy. The particular example considered there involves replacing  $\mathcal{H}$  by  $\mathcal{H}_D = -DS_z^2$ , the expression appropriate for uniaxial symmetry. This example is not only illustrative of the averaging processes encountered with single-ion Hamiltonians but serves to introduce the important distinction between the true anisotropy energy, which depends on the orientation of  $\vec{M}$ , and an apparent anisotropy energy, which depends on the orientation of  $\vec{M}_{\text{sp}}$ .

## III. MAGNETIC RESONANCE IN ISING-LIKE SYSTEM

### A. Effective Fields

Below its Néel temperature  $T_N$  of about  $3.4^\circ\text{K}$ ,

dysprosium orthophosphate is an Ising-like two-sublattice antiferromagnet<sup>9-11</sup> which exhibits a metamagnetic transition<sup>9,10</sup> and a linear magneto-electric<sup>10</sup> effect. However, the calculations of this paper are concerned with  $\text{DyPO}_4$  in its paramagnetic region and are thus applicable to the far-infrared magnetic resonance<sup>2,3</sup> experiments. We choose a rectangular coordinate system with axes  $x$ ,  $y$ ,  $z$  parallel, respectively, to the tetragonal axes  $a$ ,  $a$ ,  $c$  of the  $\text{DyPO}_4$  crystal. In accordance with the experimental conditions,<sup>2,3</sup> we assume that the crystal is exposed to a static magnetic field whose value  $H_z$  inside the crystal is sufficiently large to produce paramagnetic saturation along the  $z$  direction. We further assume

$$\mathcal{H}_{\text{eff}} = \mathcal{H}_Z + \mathcal{H}_L + \mathcal{H}_K, \quad (13)$$

where  $\mathcal{H}_Z$  is given by Eq. (3),  $\mathcal{H}_L$  denotes the Zeeman contribution arising from the local field  $\vec{H}^{\text{loc}}$ , and  $\mathcal{H}_K$  represents the anisotropic exchange interactions per ion. The fact that we neglect hyperfine effects restricts the applicability of our results to the magnetic resonance spectrum of the (approximately 56% abundant) "even" Dy isotopes.

The contributions to  $\vec{H}_{\text{eff}}$  arising from  $\mathcal{H}_Z$ ,  $\mathcal{H}_L$ , and  $\mathcal{H}_K$  will be denoted by  $\vec{H}_Z$ ,  $\vec{H}_L$ , and  $\vec{H}_K$ , respectively. We now calculate these contributions and then seek a phenomenological description of relaxation.

#### 1. Effective Magnetic Field

The discussion following Eq. (12) shows that  $\vec{H}_Z$  is given by

$$\vec{H}_Z = \frac{1}{2} \vec{g} \cdot \vec{H}, \quad (14)$$

where we now specify that  $\vec{H}$  is the magnetic field which occurs in Maxwell's equations. Thus  $\vec{H}$  includes the demagnetizing field encountered in magnetostatic problems. The  $42m$  symmetry at the  $\text{Dy}^{3+}$  sites leads to the expression

$$\vec{g} = g_1 \vec{i}_x \vec{i}_x + g_1 \vec{i}_y \vec{i}_y + g_{\parallel} \vec{i}_z \vec{i}_z, \quad (15)$$

where  $\vec{i}_x$ ,  $\vec{i}_y$ , and  $\vec{i}_z$  are unit vectors along  $x$ ,  $y$ , and  $z$ , respectively. We also note, for later reference, that Eq. (15) gives

$$\vec{g}^{-1} = g_1^{-1} \vec{i}_x \vec{i}_x + g_1^{-1} \vec{i}_y \vec{i}_y + g_{\parallel}^{-1} \vec{i}_z \vec{i}_z. \quad (16)$$

By substituting Eq. (15) into Eq. (14), we obtain

$$\vec{H}_Z = \frac{1}{2} (g_1 H_x \vec{i}_x + g_1 H_y \vec{i}_y + g_{\parallel} H_z \vec{i}_z). \quad (17)$$

#### 2. Effective Local Field

One effect of the magnetic dipole-dipole interactions is that they make a contribution (e.g., the demagnetizing field) to the magnetic field  $\vec{H}$  defined above. Another effect of these interactions is that they produce a local field  $\vec{H}^{\text{loc}}$  which exists even in a uniformly magnetized region of an unbounded

medium. It is well known that  $\vec{H}^{10c}$  may be divided into two parts, to be denoted by  $\vec{H}^{10c1}$  and  $\vec{H}^{10c2}$ , which arise, respectively, from the dipoles inside and outside the usual Lorentz sphere, and that  $\vec{H}^{10c2}$  is just the Lorentz field  $(\frac{4}{3}\pi)\vec{M}$ . In the literature, the term "local field" often refers to  $\vec{H} + \vec{H}^{10c}$  rather than to  $\vec{H}^{10c}$ .

Most analyses of magnetic resonance proceed by incorporating the field  $\vec{H}^{10c1}$  into a phenomenological "anisotropy field." The field  $\vec{H}^{10c2}$ , on the other hand, is invariably neglected on the grounds that the torque density  $\vec{M} \times \frac{4}{3}\pi\vec{M}$  is identically zero. We wish to point out, however, that in materials having  $g$ -factor anisotropy the neglect of  $\vec{H}^{10c2}$  is unjustified. This may be seen by substituting  $\frac{4}{3}\pi\vec{M}$  for  $\vec{H}$  in Eq. (10) and noting that the cross product  $\frac{2}{3}\pi(\vec{M} \cdot \vec{g}^{-1}) \times (\vec{g} \cdot \vec{M})$  does not generally vanish. (In the particular case of a magnetostatic problem involving a spherical sample,  $\vec{H}^{10c2}$  is obviously canceled out by the demagnetizing field  $-\frac{4}{3}\pi\vec{M}$ .)

Instead of decomposing  $\vec{H}^{10c}$  into  $\vec{H}^{10c1}$  and  $\vec{H}^{10c2}$ , we now introduce the expression

$$\vec{H}^{10c} = \nu_{\perp} M_x \vec{i}_x + \nu_{\perp} M_y \vec{i}_y + \nu_{\parallel} M_z \vec{i}_z, \quad (18)$$

which applies to a saturated medium possessing  $\bar{4}2m$  symmetry at the sites of the magnetic ions. The values of the coefficients  $\nu_{\parallel}$  and  $\nu_{\perp}$  for a given material (e.g.,  $\text{DyPO}_4$ ) may be obtained from calculations of appropriate dipole sums. By using Eq. (18) and treating  $\vec{H}^{10c}$  analogously to  $\vec{H}$ , we easily obtain

$$\vec{H}_L = \frac{1}{2}(g_{\perp}\nu_{\perp}M_x\vec{i}_x + g_{\perp}\nu_{\perp}M_y\vec{i}_y + g_{\parallel}\nu_{\parallel}M_z\vec{i}_z). \quad (19)$$

### 3. Effective Field Due to Anisotropic Exchange

We assume that the anisotropic exchange interactions between the  $N$  ions contained in a unit volume are represented by the Hamiltonian

$$\mathcal{H}_K^{(N)} = -\frac{1}{2} \sum' \vec{S}_i \cdot \vec{K}_{ij} \cdot \vec{S}_j, \quad (20)$$

where the tensor  $\vec{K}_{ij}$  describes the interaction between  $\text{Dy}^{3+}$  ions  $i$  and  $j$ , the "prime" indicates that the summation over  $i$  and  $j$  excludes terms involving  $i=j$ , and the factor  $\frac{1}{2}$  ensures that the interaction between ions  $i$  and  $j$  is not counted twice. Although we refer to  $\mathcal{H}_K^{(N)}$  as "anisotropic exchange," it should be noted that  $\mathcal{H}_K^{(N)}$  may contain contributions from other interactions which have the form of Eq. (20). Isotropic exchange, of course, is included in  $\mathcal{H}_K^{(N)}$ .

Next we replace  $\vec{S}_j$  by  $\langle \vec{S}_j \rangle$ , thus adopting the molecular field approximation, and assume that the spatial dependence of  $\langle \vec{S}_i \rangle$  is sufficiently gradual to justify expanding  $\langle \vec{S}_j \rangle$  about  $\langle \vec{S}_i \rangle$  to second order. If this spatial dependence is on  $y$  only, as in the experimental situation<sup>2,3</sup> and in the propagation problem of Sec. IV, then  $\langle \vec{S}_j \rangle$  becomes

$$\langle \vec{S}_j \rangle = \langle \vec{S}_i \rangle + \frac{1}{2}a \frac{\partial \langle \vec{S}_i \rangle}{\partial y} + \frac{1}{8}a^2 \frac{\partial^2 \langle \vec{S}_i \rangle}{\partial y^2}, \quad (21)$$

where  $\frac{1}{2}a$  is the separation between neighboring  $\text{Dy}^{3+}$  ions along the  $y$  axis and the spatial derivatives are to be evaluated at the  $i$ th ion. By combining Eqs. (20) and (21) and then writing  $\langle \vec{S}_i \rangle$  as  $\langle \vec{S} \rangle$ , we obtain

$$\mathcal{H}_K^{(N)} = -\frac{1}{2}N\vec{S} \cdot \vec{K} \cdot \left( 4\langle \vec{S} \rangle + \frac{1}{4}a^2 \frac{\partial^2 \langle \vec{S} \rangle}{\partial y^2} \right), \quad (22)$$

which contains the notation  $\vec{K}_{ij} = \vec{K}$  for each nearest-neighbor  $\text{Dy}^{3+}$  pair and the assumption  $\vec{K}_{ij} = 0$  for all other pairs. Also used in obtaining Eq. (22) was the fact that any given  $\text{Dy}^{3+}$  ion has four nearest neighbors which are related to each other by the  $\bar{4}2m$  symmetry of the  $\text{Dy}^{3+}$  sites, and that only two of these nearest neighbors have a nonzero separation from the given ion along the  $y$  axis. Substitution of Eq. (2) into Eq. (22) gives

$$\mathcal{H}_K^{(N)} = -\frac{1}{2}N\vec{\mu}_{sp} \cdot \vec{K} \cdot |\mu_B|^{-2} \left( \langle \vec{\mu}_{sp} \rangle + \left(\frac{1}{4}a\right)^2 \frac{\partial^2 \langle \vec{\mu}_{sp} \rangle}{\partial y^2} \right), \quad (23)$$

which we shall compare with an equivalent expression containing  $\vec{H}_K$ . To do this, we proceed in analogy with Eq. (11) and define  $\vec{H}_K$  by

$$\mathcal{H}_K = -\vec{\mu}_{sp} \cdot \vec{H}_K, \quad (24)$$

so that avoidance of double counting of the interactions leads to

$$\mathcal{H}_K^{(N)} = \frac{1}{2}N\mathcal{H}_K = -\frac{1}{2}N\vec{\mu}_{sp} \cdot \vec{H}_K, \quad (25)$$

which may be combined with Eqs. (23) and (6) to yield

$$\vec{H}_K = N^{-1} |\mu_B|^{-2} \vec{K} \cdot \left( \vec{M}_{sp} + \left(\frac{1}{4}a\right)^2 \frac{\partial^2 \vec{M}_{sp}}{\partial y^2} \right). \quad (26)$$

By using Eqs. (9) and (16) in conjunction with the expression

$$\vec{K} = K_{\perp} \vec{i}_x \vec{i}_x + K_{\perp} \vec{i}_y \vec{i}_y + K_{\parallel} \vec{i}_z \vec{i}_z, \quad (27)$$

which is appropriate for  $\bar{4}2m$  site symmetry, Eq. (26) may be written in the form

$$\vec{H}_K = \vec{H}_{K0} + \vec{H}_{K2}, \quad (28)$$

where  $\vec{H}_{K0}$  and  $\vec{H}_{K2}$  are given by

$$\begin{aligned} \vec{H}_{K0} &= \frac{2}{N|\mu_B|^2} \left( \frac{K_{\perp}M_x}{g_{\perp}} \vec{i}_x + \frac{K_{\perp}M_y}{g_{\perp}} \vec{i}_y + \frac{K_{\parallel}M_z}{g_{\parallel}} \vec{i}_z \right), \\ \vec{H}_{K2} &= \frac{a^2}{8N|\mu_B|^2} \left( \frac{K_{\perp}}{g_{\perp}} \frac{\partial^2 M_x}{\partial y^2} \vec{i}_x + \frac{K_{\perp}}{g_{\perp}} \frac{\partial^2 M_y}{\partial y^2} \vec{i}_y \right. \\ &\quad \left. + \frac{K_{\parallel}}{g_{\parallel}} \frac{\partial^2 M_z}{\partial y^2} \vec{i}_z \right). \end{aligned} \quad (30)$$

We note that if the interactions of a given  $\text{Dy}^{3+}$  ion with its next-nearest (or more distant) neighbors are nonzero, then  $\vec{H}_{K0}$  is still given by Eq.

(29) provided  $\vec{K}$  is regarded as an appropriate average over the various interactions. As to  $\vec{H}_{K2}$ , it is clear that this field does not vanish if the problem under consideration involves spin waves or other spatial variations of  $\vec{M}$ . Throughout the remainder of this paper, however, we shall use  $\vec{H}_K = \vec{H}_{K0}$  because in the relevant experiments<sup>2,3</sup>  $|\vec{H}_{K2}|$  is negligible compared to  $|\vec{H}_{K0}|$ . The reason is that under the linear conditions prevailing in these experiments, each term of Eq. (30) is smaller than the corresponding term of Eq. (29) by a factor of the order of  $(\pi\alpha/2\lambda)^2$ , where  $\lambda$  is the electromagnetic wavelength inside the sample. Since the roughness of the sample surfaces may well lead to the excitation of spin waves whose wavelength is small compared to  $\lambda$ , our use of  $\vec{H}_K = \vec{H}_{K0}$  involves the assumption that the effect of these particular spin waves is implicitly included in the phenomenological description of relaxation introduced below. Another point of interest is the absence in  $\vec{H}_K$  of first derivatives of  $\vec{M}$ . If the direction of propagation used in the experiments<sup>2,3</sup> had been  $z$  rather than  $y$  (or  $x$ ), then the  $\bar{4}2m$  site symmetry would have allowed the presence in  $\vec{H}_K$  of a term proportional to  $\partial\vec{M}/\partial z$  and leading (in conjunction with Maxwell's equations) to a nondissipative kind of attenuation of electromagnetic waves.

Collecting the various contributions to  $\vec{H}_{\text{eff}}$ , we have

$$\vec{H}_{\text{eff}} = \vec{H}_z + \vec{H}_L + \vec{H}_{K0}, \quad (31)$$

where  $\vec{H}_z$ ,  $\vec{H}_L$ , and  $\vec{H}_{K0}$  are given by Eqs. (17), (19), and (29), respectively. Substitution of Eqs. (16) and (31) into Eq. (12) then yields a particularized equation of motion which we immediately linearize. To do this, we write

$$\vec{M} = M_z \vec{i}_z + \vec{m}, \quad \vec{H} = H_z \vec{i}_z + \vec{h}, \quad (32)$$

where  $\vec{m}$  and  $\vec{h}$  are assumed to be proportional to  $e^{i\omega t}$  and to satisfy the approximations

$$|\vec{m}|/M_z \ll 1, \quad |\vec{h}|/H_z \ll 1. \quad (33)$$

Upon use of these inequalities and the abbreviation

$$H_z^{\text{an}} = 4(K_{\parallel} - K_{\perp})M_z/Ng_{\parallel}^2|\mu_B|^2, \quad (34)$$

which denotes an effective anisotropy field, the particularized equation of motion gives

$$\begin{aligned} \frac{2i\omega}{g_{\parallel}|\gamma_0|} m_x + \left[ H_z + H_z^{\text{an}} + \nu_{\parallel}M_z - \nu_{\perp}M_z \left( \frac{g_{\perp}}{g_{\parallel}} \right)^2 + \frac{i\alpha\omega}{|\gamma_0|} \right] m_y \\ = M_z \left( \frac{g_{\perp}}{g_{\parallel}} \right)^2 h_y, \quad (35) \end{aligned}$$

$$\begin{aligned} \left[ H_z + H_z^{\text{an}} + \nu_{\parallel}M_z - \nu_{\perp}M_z \left( \frac{g_{\perp}}{g_{\parallel}} \right)^2 + \frac{i\alpha\omega}{|\gamma_0|} \right] m_x - \frac{2i\omega}{g_{\parallel}|\gamma_0|} m_y \\ = M_z \left( \frac{g_{\perp}}{g_{\parallel}} \right)^2 h_x, \quad (36) \end{aligned}$$

$$m_z = 0, \quad (37)$$

where the terms containing  $\alpha$  constitute a newly introduced phenomenological description of relaxation. Our underlying assumption is that the relaxation produces an effective magnetic field which acts on  $\vec{M}_{\text{sp}}$  and is given by some negative number times  $d\vec{M}_{\text{sp}}/dt$ . This assumption is somewhat analogous to that of Gilbert<sup>12</sup> who described the relaxation in materials lacking  $g$ -factor anisotropy by introducing an effective magnetic field which acts on  $\vec{M}$  and is given by a negative number times  $d\vec{M}/dt$ . We note that Eqs. (35) and (36) contain the same  $\alpha$  and that this is a consequence of the tetragonal symmetry. On the other hand, the factor  $|\gamma_0|^{-1}$  in the  $\alpha$  terms of Eqs. (35) and (36) was inserted solely for the convenience of having the unknown parameter  $\alpha$  be positive and dimensionless.

### B. Small-Signal Susceptibility

We consider a  $\text{DyPO}_4$  sample in the form of a disk whose faces are parallel to the  $xz$  plane. The diameter of the disk is assumed to be very large compared to its thickness but very small compared to the wavelength  $\lambda$  inside the sample. In this magnetostatic limit, the fields  $h_x$  and  $H_x$  appearing in Eqs. (35) and (36) are simply the corresponding applied fields. The field  $h_y$ , on the other hand, is given by

$$h_y = -4\pi m_y, \quad (38)$$

because along the  $y$  direction the applied magnetic field is assumed to be zero. After substituting Eq. (38) into Eq. (35) and noting that the value of  $\nu_{\perp}$  is surely within the range

$$0 < \nu_{\perp} < 4\pi, \quad (39)$$

we take advantage of the Ising-like nature of  $\text{DyPO}_4$  by introducing the approximation

$$\left( \frac{4\pi M_z (g_{\perp}/g_{\parallel})^2}{H_z + H_z^{\text{an}} + \nu_{\parallel}M_z} \right)^{1/2} \ll 1, \quad (40)$$

which makes it possible to simplify Eqs. (35) and (36) by neglecting the terms involving  $(g_{\perp}/g_{\parallel})^2 m_x$  and  $(g_{\perp}/g_{\parallel})^2 m_y$ . The simplified equations (35) and (36) then yield the transverse susceptibility

$$\begin{aligned} \chi \equiv \frac{m_x}{h_x} = -M_z \left( \frac{g_{\perp}}{g_{\parallel}} \right)^2 \\ \times \frac{H_z + H_z^{\text{an}} + \nu_{\parallel}M_z + (i\alpha\omega/|\gamma_0|)}{(2\omega/g_{\parallel}|\gamma_0|)^2 - [H_z + H_z^{\text{an}} + \nu_{\parallel}M_z + (i\alpha\omega/|\gamma_0|)]^2}. \quad (41) \end{aligned}$$

Thus the static value of  $\chi$  is given by

$$\chi_{\text{stat}} = \frac{M_z (g_{\perp}/g_{\parallel})^2}{H_z + H_z^{\text{an}} + \nu_{\parallel}M_z}, \quad (42)$$

which shows that the approximation (40) may be expressed in the alternative form

$$(4\pi\chi_{\text{stat}})^{1/2} \ll 1. \quad (43)$$

Next we note that if the undamped resonance frequency (i. e., the resonance frequency for  $\alpha=0$ ) is to have the value  $\omega$ , then  $H_z$  must have that value  $H_z^{\text{res}}$  which satisfies

$$\omega = \frac{1}{2}g_{\parallel}|\gamma_0|(H_z^{\text{res}} + H_z^{\text{an}} + \nu_{\parallel}M_z). \quad (44)$$

The resonance condition (44) is inapplicable, of course, unless  $\omega$  exceeds  $\frac{1}{2}g_{\parallel}|\gamma_0|(H_z^{\text{an}} + \nu_{\parallel}M_z)$ . With the use of Eqs. (34), (9), (6), (2), (15), and (5), Eq. (44) may be written as

$$\hbar\omega = g_{\parallel}|\mu_B|(H_z^{\text{res}} + \nu_{\parallel}M_z) - 4(K_{\parallel} - K_{\perp})\langle S_z \rangle, \quad (45)$$

where  $M_z$  is given by

$$M_z = -Ng_{\parallel}|\mu_B|\langle S_z \rangle. \quad (46)$$

In the case of  $\text{DyPO}_4$ , the lowest-lying energy levels are known to constitute an exchange- and dipole-split Kramers doublet<sup>9</sup> whose separation from the nearest excited level is rather large<sup>13</sup> ( $\approx 70 \text{ cm}^{-1}$ ), being about ten times the doublet splitting. Even at a temperature as high as the  $4.2^\circ \text{K}$  used in the far-infrared magnetic resonance<sup>2,3</sup> experiments, therefore,  $\text{DyPO}_4$  may be described accurately by a fictitious spin  $S$  of  $\frac{1}{2}$ . If  $H_z$  is sufficiently large to cause paramagnetic saturation, then only the lower level of the ground doublet is occupied. Thus we have  $\langle S_z \rangle = -\frac{1}{2}$ , because it is known from the observed<sup>13</sup> linearity of the Zeeman splitting that even at the large values of  $H_z$  used in the resonance experiments<sup>2,3</sup> the description based on  $S = \frac{1}{2}$  does remain valid. Equation (45) now becomes

$$\hbar\omega = g_{\parallel}|\mu_B|(H_z^{\text{res}} + \nu_{\parallel}M_z) + 2(K_{\parallel} - K_{\perp}), \quad (47)$$

which agrees (for  $K_{\perp} = 0$ ) with the resonance condition proposed and used in conjunction with the experiments.<sup>2,3</sup>

To simplify Eq. (41) for the susceptibility, we define  $\delta H_z$  by

$$\delta H_z = \alpha\omega/|\gamma_0|, \quad (48)$$

which will turn out to be [see Eq. (51)] the half-width of the resonance at half-maximum absorption. After substituting Eqs. (44) and (48) as well as the identity  $H_z = H_z^{\text{res}} + (H_z - H_z^{\text{res}})$  into Eq. (41), we introduce the approximations

$$\frac{|H_z - H_z^{\text{res}}|}{H_z^{\text{res}} + H_z^{\text{an}} + \nu_{\parallel}M_z} \ll 1, \quad (49)$$

$$\frac{\delta H_z}{H_z^{\text{res}} + H_z^{\text{an}} + \nu_{\parallel}M_z} \ll 1, \quad (50)$$

and find that Eq. (41) may now be replaced by

$$\chi = \frac{\frac{1}{2}M_z(g_{\perp}/g_{\parallel})^2 [(H_z - H_z^{\text{res}})/\delta H_z] - i}{\delta H_z} \frac{1}{1 + [(H_z - H_z^{\text{res}})/\delta H_z]^2}$$

$$+ \frac{\frac{1}{4}M_z(g_{\perp}/g_{\parallel})^2}{H_z^{\text{res}} + H_z^{\text{an}} + \nu_{\parallel}M_z}. \quad (51)$$

The validity of the result (51) is clearly limited to frequencies which are sufficiently high to make Eq. (44) applicable.

As to the approximations (49) and (50), their meaning is that both the "excursion" from the actual resonance field and the half-width of the resonance are small compared to the effective resonance field. We also note that the inequality (40) is the most stringent approximation made so far. By combining the inequalities (49) and (40), the latter may be expressed in the more useful form

$$\left( \frac{4\pi M_z(g_{\perp}/g_{\parallel})^2}{H_z^{\text{res}} + H_z^{\text{an}} + \nu_{\parallel}M_z} \right)^{1/2} \ll 1. \quad (52)$$

The quantity of interest in the propagation problem to be treated in Sec. IV is not the susceptibility  $\chi$  but the permeability

$$\mu_p = 1 + 4\pi\chi, \quad (53)$$

where the purpose of the subscript  $p$  is to prevent the permeability from being confused with the ionic magnetic moment. By using the approximation (52) in conjunction with Eqs. (53) and (51), we see that the  $\delta H_z$ -free term of Eq. (51) is negligible when used in  $\mu_p$  rather than in  $\chi$ .

Thus we obtain

$$\mu_p = \mu_1 - i\mu_2 = 1 + (\mu_1 - 1) - i\mu_2, \quad (54)$$

$$\mu_1 - 1 = \frac{2\pi M_z(g_{\perp}/g_{\parallel})^2}{\delta H_z} \frac{(H_z - H_z^{\text{res}})/\delta H_z}{1 + [(H_z - H_z^{\text{res}})/\delta H_z]^2}, \quad (55a)$$

$$\mu_2 = \frac{2\pi M_z(g_{\perp}/g_{\parallel})^2}{\delta H_z} \frac{1}{1 + [(H_z - H_z^{\text{res}})/\delta H_z]^2}. \quad (55b)$$

Since the quantity required in Sec. IV is actually  $\mu_p^{1/2}$ , it is useful to introduce our final and most stringent approximation

$$\frac{2\pi M_z(g_{\perp}/g_{\parallel})^2}{\delta H_z} \ll 1, \quad (56)$$

whose meaning is that the Ising-like aspect of the material under consideration is more pronounced than the smallness of its linewidth. Because of the inequality (56), the  $|\mu_1 - 1|$  and  $|\mu_2|$  of Eqs. (55) are now small quantities so that Eq. (54) yields

$$\mu_p^{1/2} = 1 + \frac{1}{2}(\mu_1 - 1 - i\mu_2). \quad (57)$$

#### IV. ELECTROMAGNETIC PROPAGATION IN ISING-LIKE SYSTEM

##### A. Propagation Constant and Characteristic Impedance

Instead of the magnetostatic approximation of Sec. III B, we now use the Maxwell equations

$$c\vec{\nabla} \times \vec{e} = -\frac{\partial(\vec{h} + 4\pi\vec{m})}{\partial t}, \quad (58a)$$

$$c\vec{\nabla} \times \vec{h} = \frac{\partial(\vec{\epsilon} \cdot \vec{e})}{\partial t}, \quad (58b)$$

and express the dielectric constant  $\vec{\epsilon}$  in the form

$$\vec{\epsilon} = \epsilon_{\perp} \vec{i}_x \vec{i}_x + \epsilon_{\perp} \vec{i}_y \vec{i}_y + \epsilon_{\parallel} \vec{i}_z \vec{i}_z, \quad (59)$$

which is appropriate for the 4/*mmm* macroscopic symmetry of DyPO<sub>4</sub>. Assuming the entire space and time dependence of  $\vec{m}$ ,  $\vec{h}$ , and  $\vec{e}$  to be given by  $e^{i\omega t - ky}$ , we find that Eqs. (58) yield

$$[1 + (k^2/k_0^2 \epsilon_{\parallel})] h_x = -4\pi m_x, \quad (60a)$$

$$h_y = -4\pi m_y, \quad (60b)$$

$$[1 + (k^2/k_0^2 \epsilon_{\perp})] h_z = -4\pi m_z, \quad (60c)$$

$$e_x = -(k/ik_0 \epsilon_{\perp}) h_z, \quad (61a)$$

$$e_y = 0, \quad (61b)$$

$$e_z = (k/ik_0 \epsilon_{\parallel}) h_x, \quad (61c)$$

where the abbreviation

$$k_0 = \omega/c = 2\pi/\lambda_0 \quad (62)$$

denotes the absolute magnitude of the propagation constant in free space. Equations (60) are seen to have a solution for which  $h_x = h_y = \vec{m} = 0$  and  $h_z \neq 0$ . We assume, however, that this "nonmagnetic" wave (characterized by  $k = ik_0 \epsilon_{\perp}^{1/2}$ ) is not excited under the experimental conditions, and we shall henceforth be concerned only with that wave for which  $h_x = 0$ . Thus Eq. (60c) gives  $m_z = 0$ , in agreement with Eq. (37). By eliminating  $h_x$  and  $h_y$  from Eqs. (60a), (60b), (35), and (36), we then obtain two linear homogeneous equations for the unknowns  $m_x$  and  $m_y$ . In order that these equations possess a nonvanishing solution, the determinant of the coefficients must vanish. This requirement yields a secular equation which we simplify by using the inequality (39) in conjunction with the approximation (40). The solution of the secular equation is

$$-\frac{k^2}{k_0^2 \epsilon_{\parallel}} = 1 - 4\pi M_x \left( \frac{g_{\perp}}{g_{\parallel}} \right)^2 \times \frac{H_x + H_x^{\text{an}} + \nu_{\parallel} M_x + (i\alpha\omega/|\gamma_0|)}{(2\omega/g_{\parallel} |\gamma_0|)^2 - [H_x + H_x^{\text{an}} + \nu_{\parallel} M_x + (i\alpha\omega/|\gamma_0|)]^2}, \quad (63)$$

which may be combined with Eq. (41) to give

$$k = ik_0 [\epsilon_{\parallel} (1 + 4\pi\chi)]^{1/2}. \quad (64)$$

We wish to emphasize that the susceptibility  $\chi$  contained in Eq. (64) is the  $\chi$  given by Eq. (41). Thus Eq. (64) does not yet contain the approximations (49), (50), and (56). In situations where these approximations are not fulfilled, therefore, the solution of the boundary value problem of Sec. IV B should be based on Eq. (64) rather than on the approximate expression

$$k = ik_0 \epsilon_{\parallel}^{1/2} [1 + \frac{1}{2}(\mu_1 - 1 - i\mu_2)], \quad (65)$$

which results from combining Eqs. (64), (53), and (57). The advantage of Eq. (65) is that it contains the simple expressions for  $\mu_1 - 1$  and  $\mu_2$  which are given by Eqs. (55) and are subject to the approximation (56). In the problem of Sec. IV B, therefore, we use the propagation constant  $k$  of Eq. (65) rather than that of Eq. (64). Thus we avoid the need for computer calculations and obtain a result in closed form. Also used in Sec. IV B is the ratio  $Z = e_z/h_x$  whose value

$$Z = e_z/h_x = k/ik_0 \epsilon_{\parallel} \quad (66)$$

is given by Eq. (61c) and is proportional to the characteristic impedance of the material under consideration. For a wave propagating along  $-\vec{i}_y$ , rather than  $+\vec{i}_y$ , the sign of  $k$  and hence that of  $Z$  must be reversed.

### B. Resonant Transmission through Slab

We suppose that the DyPO<sub>4</sub> sample is in the form of a slab bounded by the planes  $y=0$  and  $y=L$  along the  $y$  direction but unbounded along the  $x$  and  $z$  directions. Suppressing, for simplicity, the time dependence  $e^{i\omega t}$ , we now consider the magnetic components of the five waves which are involved in propagation through the slab. The incident wave  $h_{x0}^{(1)} e^{-ik_0 y}$  and the reflected wave  $h_{x0}^{(2)} e^{ik_0 y}$  propagate in "front" of the slab ( $y < 0$ ), the waves  $h_{x0}^{(3)} e^{-ky}$  and  $h_{x0}^{(4)} e^{ky}$  propagate inside the slab ( $0 \leq y \leq L$ ), and the transmitted wave  $h_{x0}^{(5)} e^{-ik_0 y}$  propagates in "back" of the slab ( $y > L$ ). It should be noted that the corresponding electric components are given by Eq. (66), that the amplitudes  $h_{x0}^{(1)} \dots h_{x0}^{(5)}$  are, in general, complex, and that the quantity of interest is the relative amplitude

$$\tau = h_{x0}^{(5)} / h_{x0}^{(1)}. \quad (67)$$

The boundary conditions require that both  $e_z$  and  $h_x$  be continuous at  $y=0$  as well as at  $y=L$ . Thus we obtain

$$h_{x0}^{(1)} - h_{x0}^{(2)} - Z h_{x0}^{(3)} + Z h_{x0}^{(4)} = 0, \quad (68a)$$

$$h_{x0}^{(1)} + h_{x0}^{(2)} - h_{x0}^{(3)} - h_{x0}^{(4)} = 0, \quad (68b)$$

$$-\tau e^{-ik_0 L} h_{x0}^{(1)} + Z e^{-kL} h_{x0}^{(3)} - Z e^{kL} h_{x0}^{(4)} = 0, \quad (68c)$$

$$-\tau e^{-ik_0 L} h_{x0}^{(1)} + e^{-kL} h_{x0}^{(3)} + e^{kL} h_{x0}^{(4)} = 0, \quad (68d)$$

which may be regarded as four linear homogeneous equations for the unknowns  $h_{x0}^{(1)}$ ,  $h_{x0}^{(2)}$ ,  $h_{x0}^{(3)}$ , and  $h_{x0}^{(4)}$ . In order that these equations possess a nonvanishing solution, the determinant of the coefficients must vanish. This requirement yields a secular equation whose solution is

$$\tau = \frac{4Z e^{ikh_0 L}}{(1+Z)^2 e^{kL} - (1-Z)^2 e^{-kL}}. \quad (69)$$

We note parenthetically that if the spin-wave terms discussed and discarded in Sec. III A were non-

negligible, then it would be necessary to use the general exchange boundary condition<sup>14</sup> in addition to the electromagnetic boundary condition used above.

The quantity of interest in the experiments<sup>2,3</sup> is the ratio of the transmitted intensity to the incident intensity. This quantity is given by  $T = |\tau|^2$  because the intensity is the time average of the magnitude of the Poynting vector. Since the quantity actually measured<sup>2,3</sup> is not equal to  $T$  but proportional to  $T$ , we calculate not the relative transmission  $T$  but its normalized value  $T/T_\infty$ , where  $T_\infty$  is the value of  $T$  for  $\mu_1 - 1 = \mu_2 = 0$ , i. e., for  $H_z = \infty$ . In calculating  $\tau$  and hence  $T/T_\infty$  from Eq. (69), we use Eqs. (65) and (66) and recall that [because of the approximation (56)] both  $|\mu_1 - 1|$  and  $|\mu_2|$  are small compared to unity. We find it convenient, moreover, to assume that  $\epsilon_{\parallel}$  is real and that its value satisfies  $\epsilon_{\parallel} \gtrsim \frac{9}{4}$ . These restrictions are introduced solely for the sake of simplicity and can be removed, if necessary, at a later date. After some lengthy algebra we obtain our final result

$$\frac{T}{T_\infty} = \frac{A}{D} \left( 1 + \frac{B\rho}{D} (\mu_1 - 1) + \frac{C\rho}{D} \mu_2 \right) e^{-k_\epsilon L \mu_2}, \quad (70)$$

where the abbreviations  $A$ ,  $B$ ,  $C$ ,  $D$ ,  $\rho$ , and  $k_\epsilon$  are defined by

$$A = \rho^4 - 2\rho^2 \cos 2k_\epsilon L + 1, \quad (71a)$$

$$B = \rho^2 - (1 + \rho^2) e^{-k_\epsilon L \mu_2} \cos\{2k_\epsilon L [1 + \frac{1}{2}(\mu_1 - 1)]\} + e^{-2k_\epsilon L \mu_2}, \quad (71b)$$

$$C = (\rho^2 - 1) e^{-k_\epsilon L \mu_2} \sin\{2k_\epsilon L [1 + \frac{1}{2}(\mu_1 - 1)]\}, \quad (71c)$$

$$D = \rho^4 - 2\rho^2 e^{-k_\epsilon L \mu_2} \cos\{2k_\epsilon L [1 + \frac{1}{2}(\mu_1 - 1)]\} + e^{-2k_\epsilon L \mu_2}, \quad (71d)$$

$$\rho = (\epsilon_{\parallel}^{1/2} + 1) / (\epsilon_{\parallel}^{1/2} - 1), \quad (71e)$$

$$k_\epsilon = k_0 \epsilon_{\parallel}^{1/2}. \quad (71f)$$

Of particular interest is the limiting case of a thin sample. Since in this case  $L$  is small compared to the wavelength  $\lambda$  inside the slab, it is appropriate to introduce into Eq. (70) the additional approximation

$$2k_\epsilon L \ll 1. \quad (72)$$

Equation (70) now becomes

$$T/T_\infty = 1, \quad (73)$$

which shows that in a thin sample of a strongly Ising-like material the deviation of  $T/T_\infty$  from unity vanishes in first order. This conclusion is a quantitative confirmation of our earlier remark (see Sec. I) concerning the possibility that in a thin sample of an Ising-like material the resonance absorption is too weak to be observable. We wish to emphasize, however, that the validity of Eq.

(73) is confined to materials which are so strongly Ising-like that the stringent approximation (56) is satisfied.

In order to derive a thin sample result in which the first-order deviation of  $T/T_\infty$  from unity is nonvanishing, we return to Eq. (69) and use the  $k$  of Eq. (64) rather than that of Eq. (65). Thus we avoid the assumption  $|\mu_p - 1| \ll 1$  which follows from the approximation (56) and Eqs. (55). We assume, instead, that  $k_0 L$ ,  $\epsilon_{\parallel}$ , and  $\mu_p$  satisfy the approximations

$$|kL| = k_0 L |(\epsilon_{\parallel} \mu_p)^{1/2}| \ll 1, \quad (74a)$$

$$\frac{1}{2} k_0 L |\epsilon_{\parallel} + \mu_p| \ll 1, \quad (74b)$$

and find that Eq. (69) now yields

$$T/T_\infty = 1 - k_0 L \mu_2, \quad (75)$$

which does contain a first-order deviation from unity. If we now express  $\mu_2$  by Eq. (55b), then we find that this deviation is an even function of  $H_z - H_z^{\text{res}}$ , i. e.,  $T/T_\infty$  is symmetrical, and if we take the further step of invoking the approximation (56), then we again obtain Eq. (73).

Next to be discussed is Eq. (70), our result for the general case of an arbitrary  $L$ . We consider, for this purpose, the typical graphs of  $T/T_\infty$  shown in Fig. 1. They were computed on the basis of Eq. (70) and the following representative values<sup>3</sup> of the various parameters:  $k_0 = 2\pi/0.022023 \text{ cm}^{-1}$ ;  $\epsilon_{\parallel} = 16.8$ ;  $M_z = 693.30 \text{ emu}$ ;  $g_{\parallel} = 19.29$ ;  $g_{\perp} = 0.10$ ;  $\delta H_z = 12.5 \text{ Oe}$ . [As to the value of  $M_z$ , note that Eq. (46) gives  $M_z = 1234.9$  if we use  $g_{\parallel} = 19.29$ ,  $\langle S_z \rangle = -\frac{1}{2}$ , unit-cell volume =  $289.61 \times 10^{-24} \text{ cm}^3$ , and number of  $\text{Dy}^{3+}$  ions/unit cell = 4. Correcting for the 56.142% relative abundance of the "even" Dy isotopes then yields the value  $M_z = 693.30$  assumed in the computation. It may be more realistic, however, to use the total  $M_z$ , i. e.,  $M_z = 1234.9$ , because in the present calculation hyperfine effects have been neglected. The upper part of Fig. 1 shows  $T/T_\infty$  as a function of  $L$  for a fixed value of  $H_z$ , namely, for  $H_z = H_z^{\text{res}}$ , and clearly displays a pattern of dimensional resonances indicative of interference effects. The lower part of Fig. 1 shows  $T/T_\infty$  as a function of  $H_z - H_z^{\text{res}}$  for  $L = L_1 = 0.0410 \text{ cm}$  (left-hand portion) and for  $L = L_2 = 0.0420 \text{ cm}$  (right-hand portion). It is seen that for  $L = L_1$ , a thickness for which  $d(T/T_\infty)/dL$  is positive, the magnetic resonance transmission is such that  $|d(T/T_\infty)/d(H_z - H_z^{\text{res}})|$  is larger for  $H_z - H_z^{\text{res}} < 0$  than for  $H_z - H_z^{\text{res}} > 0$ , whereas for  $L = L_2$ , a thickness for which  $d(T/T_\infty)/dL$  is negative, the magnetic resonance transmission is such that  $|d(T/T_\infty)/d(H_z - H_z^{\text{res}})|$  is larger for  $H_z - H_z^{\text{res}} > 0$  than for  $H_z - H_z^{\text{res}} < 0$ . These asymmetries do not occur in the thin sample result of Eq. (75) and are, therefore, consequences of electromagnetic propagation effects. Specific-



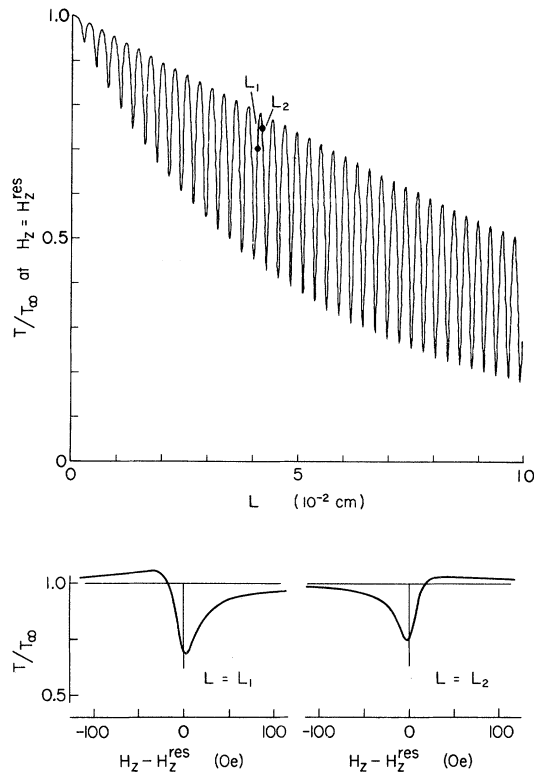


FIG. 1. Graphs of the normalized relative transmission  $T/T_\infty$  computed on the basis of Eq. (70) and the representative values of the various parameters listed in the text. Upper part:  $T/T_\infty$  vs sample thickness  $L$  for  $H_z = H_z^{\text{res}}$ , i. e., at magnetic resonance. Lower part:  $T/T_\infty$  vs  $H_z - H_z^{\text{res}}$  for  $L = L_1$  (left-hand portion) and for  $L = L_2$  (right-hand portion).

ly, these asymmetries arise from the fact that in Eq. (70) the deviation of  $T/T_\infty$  from unity is due not only to  $\mu_2$  but also to  $\mu_1 - 1$ , and that at resonance  $\mu_1 - 1$  changes sign. It should be noted, in this connection, that in Eq. (70) the quantity  $\mu_1 - 1$  occurs both by itself and as part of the phase angle  $2k_z L [1 + \frac{1}{2}(\mu_1 - 1)]$ , corresponding to the fact that  $\mu_1 - 1$  is contained both in  $Z$  and in  $k$ . But the most revealing aspect of Eq. (70) is probably its prediction that under appropriate conditions  $T/T_\infty$  can exceed unity. This prediction constitutes a particularly clear manifestation of electromagnetic propagation effects. The reason is that in the absence of such effects, i. e., in the thin sample result of Eq. (75), the occurrence of  $T/T_\infty > 1$  is impossible because it would require that  $\mu_2$  be negative and hence that energy be generated rather than absorbed in the sample.

We close with some comments on the relevance of Eq. (70) to the far-infrared magnetic resonance experiments<sup>2,3</sup> in  $\text{DyPO}_4$ . First to be noted is the fact that the experimental results<sup>2,3</sup> can be fitted reasonably well with asymmetric curves of the type

shown in Fig. 1 for  $L = L_1$ . Thus it appears that electromagnetic propagation effects offer a possible explanation of the asymmetry of the resonance. We wish to stress, however, that a successful fitting of the experimental curves by means of Eq. (70) merely suggests but does not conclusively demonstrate the presence of propagation effects. The reason is that the thickness of the presently available  $\text{DyPO}_4$  crystals is rather nonuniform, a situation which perhaps can be ameliorated by the development of a polishing technique suitable for crystals of unusual brittleness. For a given crystal, the measured value of  $L$  varies, in fact, by as much as  $20 \mu$  (which is 5–10% of  $L$ ) over the sample surface. On the other hand, a change of only  $10 \mu$  in the value of  $L$  used in Eq. (70) is sufficient to change the asymmetry of the calculated  $T/T_\infty$  vs  $H_z - H_z^{\text{res}}$  curve from that shown in Fig. 1 for  $L = L_1$  to that shown in Fig. 1 for  $L = L_2$ . It is conceivable, therefore, that the variations in the sample thickness cause an averaging of the two kinds of asymmetry, and that the observed asymmetry arises from processes not included in the present theory. Two examples of such processes are the scattering of electromagnetic (or spin) waves by the “steps” on the sample surfaces and some suitable linewidth mechanism capable of producing an asymmetric line shape even in a thin sample. In view of the uncertainties resulting from sample imperfections, we suggest that the observation most amenable to theoretical interpretation is not the line-shape asymmetry but the experimental result that  $T/T_\infty$  can exceed unity. A probably unique explanation of this experimental result is offered by the presence of propagation effects, as shown by the above-mentioned fact that under appropriate conditions Eq. (70) does predict  $T/T_\infty > 1$ . It should also be noted that while our calculations are directly applicable to  $\text{DyPO}_4$  in a state of paramagnetic saturation, the methods of the present paper are clearly adaptable to other Ising-like materials, including antiferromagnets and ferrimagnets in which the  $g$  tensors of the various sublattices may all be different.

#### ACKNOWLEDGMENTS

The author wishes to thank G. A. Prinz for many discussions of experimental results, and both him and J. H. Schelleng for programming an electronic computer to plot Fig. 1 and other graphs of Eq. (70).

#### APPENDIX

As stated toward the end of Sec. II, we now derive the classical equation of motion of  $\vec{M}$  for the situation in which the  $\mathcal{H}$  of Eq. (1) is replaced by

$$\mathcal{H}_D = -DS_z^2. \quad (\text{A1})$$

We use a rectangular coordinate system  $x, y, z$  whose  $z$  axis is along the principal axis of the crystal. Next we write the equations describing the  $x, y, z$  components of Eq. (1) and apply the commutation relations  $\vec{S} \times \vec{S} = i\vec{S}$ . Assuming the existence of a ferromagnetic exchange interaction which produces a nonvanishing  $\langle \vec{\mu}_{sp} \rangle$ , we then introduce the transformation

$$S_x = S_\xi \cos \varphi - S_\eta \cos \theta \sin \varphi + S_\zeta \sin \theta \sin \varphi, \quad (\text{A2a})$$

$$S_y = S_\xi \sin \varphi + S_\eta \cos \theta \cos \varphi - S_\zeta \sin \theta \cos \varphi, \quad (\text{A2b})$$

$$S_z = S_\eta \sin \theta + S_\zeta \cos \theta, \quad (\text{A2c})$$

where the  $\zeta$  axis of the  $\xi, \eta, \zeta$  coordinate system is taken to be along  $\langle \vec{\mu}_{sp} \rangle$ . We further suppose the anisotropy energy to be much smaller than the exchange energy so that the quantum-mechanical portion of the calculation of average values may be based on first-order perturbation theory. By taking the  $\zeta$  axis to be the axis of quantization, one easily obtains the well-known relations<sup>7</sup>

$$\langle S_\xi^2 \rangle = \langle S_\eta^2 \rangle = -\frac{1}{2}[\langle S_\zeta^2 \rangle - S(S+1)], \quad (\text{A3a})$$

$$\langle S_\xi S_\eta + S_\eta S_\xi \rangle = \langle S_\xi S_\zeta \rangle = \langle S_\eta S_\zeta \rangle = 0. \quad (\text{A3b})$$

A straightforward calculation based on Eqs. (A1)–(A3) with the use of Eqs. (2), (5), and (6) then yields

$$\frac{\gamma_0^{-1} d\vec{M}_{sp}}{dt} = \vec{M}_{sp} \times \vec{H}_D, \quad (\text{A4})$$

where  $\vec{H}_D$  is given by

$$\vec{H}_D = -2(K_{sp})_1 (M_{sp})_z \vec{i}_z / M_{sp}^2. \quad (\text{A5})$$

Here  $\vec{i}_z$  is a unit vector along the  $z$  axis and  $(K_{sp})_1$  is, at this point, merely an abbreviation for the quantity

$$(K_{sp})_1 = -\frac{1}{2}ND[3\langle S_\zeta^2 \rangle - S(S+1)]. \quad (\text{A6})$$

To eliminate  $\vec{M}_{sp}$  and its components from Eqs. (A4) and (A5), we use Eq. (9) and the expression

$$\vec{g} = g_1 \vec{i}_x \vec{i}_x + g_1 \vec{i}_y \vec{i}_y + g_1 \vec{i}_z \vec{i}_z, \quad (\text{A7})$$

which is appropriate for certain cases involving uniaxial symmetry. Thus we obtain

$$\vec{M}_{sp} = 2(g_1^{-1} M_x \vec{i}_x + g_1^{-1} M_y \vec{i}_y + g_1^{-1} M_z \vec{i}_z), \quad (\text{A8})$$

where  $\vec{i}_x$  and  $\vec{i}_y$  are defined analogously to  $\vec{i}_z$ . Equation (A5) now becomes

$$\vec{H}_D = -\frac{g_1 (K_{sp})_1 M_z \vec{i}_z}{g_1^2 M^2 - (g_1^2 - g_1^2) M_z^2}, \quad (\text{A9})$$

which is seen to reduce to

$$\vec{H}_D = -[g_1 (K_{sp})_1 / M] \vec{i}_z \quad (\text{A10})$$

in the important special case when the displacement of  $\vec{M}_{sp}$  from its equilibrium position is small. Substitution of Eqs. (A8) and (A9) into Eq. (A4) then yields our final equation of motion for the situation described by  $\mathcal{H} = \mathcal{H}_D$ . While we do not present this final equation explicitly, we note that it can be written in the compact form of Eq. (12) in which  $\vec{H}_{eff}$  is now given by the  $\vec{H}_D$  of Eq. (A9).

Two comments on the above treatment seem appropriate. The first of these concerns the meaning of  $(K_{sp})_1$ . With the help of Eqs. (A1)–(A3) we obtain the well-known expression<sup>7</sup>

$$N\langle \mathcal{H}_D \rangle = -\frac{1}{2}ND[3\langle S_\zeta^2 \rangle - S(S+1)] \cos^2 \theta \quad (\text{A11})$$

for that portion of the anisotropic part of the free energy density which arises from the single-ion anisotropy represented by  $\mathcal{H}_D$ . Substitution of Eq. (A6) into Eq. (A11) gives

$$N\langle \mathcal{H}_D \rangle = (K_{sp})_1 \cos^2 \theta, \quad (\text{A12})$$

so that  $(K_{sp})_1$  is just the first-order anisotropy constant arising from  $\mathcal{H}_D$ . We wish to emphasize that if  $\vec{g}$  is anisotropic then  $(K_{sp})_1$  should not be identified with the total (i. e., phenomenological) first-order anisotropy constant  $K_1$ . This is not only because  $(K_{sp})_1$  contains solely that portion of the anisotropy which arises from  $\mathcal{H}_D$ , but also because of the fact that the anisotropy energy density  $N\langle \mathcal{H}_D \rangle$  depends on the orientation of  $\vec{M}_{sp}$  whereas the total anisotropy energy density depends on the orientation of  $\vec{M}$ .

The second comment on the treatment given in this Appendix concerns the fact that it employs first-order perturbation theory. This is usually adequate in the case of uniaxial symmetry. In the case of lower symmetry (e. g., orthorhombic), however, the use of higher-order perturbation theory was shown<sup>15</sup> to reveal a new effect, namely, a mutual admixture of the various spin states and hence an anisotropic  $\vec{M}_{sp}$ . This effect differs, of course, from the case of an anisotropic  $\vec{M}$  treated in the present paper. Since the anisotropy of  $\vec{M}_{sp}$  is not yet of experimental importance, its dynamical consequences will not be considered here.

<sup>1</sup>J. Boettcher, K. Dransfeld, and K. F. Renk, Phys. Letters **26A**, 146 (1968); J. P. Kotthaus and K. Dransfeld, *ibid.* **30A**, 34 (1969).

<sup>2</sup>G. A. Prinz and R. J. Wagner, Phys. Letters **30A**, 520 (1969).

<sup>3</sup>G. A. Prinz and R. J. Wagner, J. Appl. Phys. **42**, 1569 (1971), abstract.

<sup>4</sup>G. T. Rado, J. Appl. Phys. **42**, 1570 (1971), abstract;

explicit mention of the local field contribution to the Hamiltonian was omitted for brevity.

<sup>5</sup>M. H. L. Pryce, Phys. Rev. Letters **3**, 375 (1959).

<sup>6</sup>A. G. Gurevich, V. A. Sanina, E. I. Golovenchits, and S. S. Starobinets, J. Appl. Phys. **40**, 1512 (1969).

<sup>7</sup>T. Nagamiya, K. Yosida, and R. Kubo, in *Advances in Physics*, edited by N. F. Mott (Taylor and Francis, London, 1955), Vol. 4, p. 1.

<sup>8</sup>See, for example, E. A. Turov, *Physical Properties of Magnetically Ordered Crystals* (Academic, New York, 1965), p. 98; F. K. Kneubühl, *Helv. Phys. Acta* **35**, 259 (1962). However, A. Abragam and B. Bleaney [*Electron Paramagnetic Resonance of Transition Ions* (Clarendon, Oxford, England, 1970), pp. 650–653], showed that in the case where  $\tilde{S}$  is the fictitious spin  $\frac{1}{2}$  of a Kramers doublet rather than some true spin, the question whether  $\tilde{g}$  is symmetric is of little importance because in this case the  $g$  factor can always be represented by a tensor which is diagonal.

<sup>9</sup>J. C. Wright and H. W. Moos, *Phys. Letters* **29A**, 495 (1969).

<sup>10</sup>G. T. Rado, *Phys. Rev. Letters* **23**, 644 (1969); **23**, 946(E) (1969); *Solid State Commun.* **8**, 1349 (1970).

<sup>11</sup>J. H. Colwell, B. Mangum, D. D. Thornton, J. C.

Wright, and H. W. Moos, *Phys. Rev. Letters* **23**, 1245 (1969).

<sup>12</sup>T. L. Gilbert, Armour Research Foundation Report, May, 1956 (unpublished); an abstract appeared in *Phys. Rev.* **100**, 1243 (1955). See also C. W. Haas and H. B. Callen, in *Magnetism*, edited by G. T. Rado and H. Suhl (Academic, New York, 1963), Vol. I, p. 466.

<sup>13</sup>G. A. Prinz (unpublished).

<sup>14</sup>G. T. Rado and J. R. Weertman, *J. Phys. Chem. Solids* **11**, 315 (1959), Eqs. (15) and (17). The necessity for introducing additional boundary conditions in the presence of exchange effects was first pointed out by W. S. Ament and G. T. Rado, *Phys. Rev.* **97**, 1558 (1955).

<sup>15</sup>G. T. Rado, *Phys. Rev.* **176**, 644 (1968); **184**, 606(E) (1969).

## Soft-Phonon Couplings in the Pressure-Induced Phase Transition in SbSI

M. K. Teng, M. Balkanski, and M. Massot

*Laboratoire de Physique des Solides, Université Paris VI, 9, Quai Saint Bernard, Paris, France*

(Received 21 June 1971)

The Raman spectra of the soft-phonon behavior in the ferroelectric transition in SbSI is studied by means of a new technique in which the phase transition is induced by hydrostatic pressure. The crystal temperature is maintained constant and the ferroelectric transition is created by a linear shift of the Curie temperature. Evidence is provided for the existence of two distinct mode couplings involving three phonons.

### INTRODUCTION

Antimony sulfo-iodide is a crystal in which there coexist a large number of remarkable physical properties. SbSI is the first semiconductor found to be both photoconductive and also ferroelectric.<sup>1,2</sup> In addition, the crystal exhibits a strong electro-optical and electromechanical effect<sup>3</sup> and an unusually strong dependence of the band gap on the electric field,<sup>4</sup> as well as a very strong energy band-gap variation with temperature.<sup>5</sup> All these interesting properties superpose and vary substantially when the temperature changes, in particular around the Curie temperature  $T_C$ . In previous Raman-scattering investigations, it was reported that an optical  $\Gamma_1(A_1)$  band shows a soft-mode behavior when  $T_C$  is approached from below.<sup>6</sup> It was also proposed that the band consists in fact of two optical modes which exhibit the level-repulsion characteristic for a system of coupled harmonic oscillators.<sup>7,8</sup> Infrared reflectivity measurements<sup>9</sup> show a temperature-dependent optical mode when  $T_C$  is approached from above. All these experiments were performed at various temperatures which modify simultaneously and appreciably the other fundamental properties of the crystal.

In this paper, we propose a different technique

to study the phonon spectrum change during the phase transition in SbSI. Under hydrostatic pressure, the Curie temperature  $T_C$  is considerably lowered:  $dT_C/dP \approx -39$  to  $-50$  °C/kbar, according to Refs. 5 and 10, and  $dT_C/dP \approx -37$  °C/kbar, according to Ref. 11. It is then expected that the ferroelectric transition may be induced by hydrostatic pressure at fixed temperature. The phonon behavior may therefore be studied at various  $T_C$  instead of  $T$ . This method presents the significant advantage of eliminating the influence of most of the other effects, since they are only slightly pressure dependent. Furthermore, with our experimental equipment an error of  $\Delta P = 20$  bar on pressure is estimated; this corresponds to an error of about  $\Delta T_C = 0.8$  °C on the Curie temperature. It is then possible to study the phase transition with more accuracy.

It is the purpose of this paper to present the Raman scattering of SbSI investigated at a set of fixed temperatures under hydrostatic pressure. Our attention is especially focused on the ferroelectric phase-transition region where substantial spectral change is expected. The results deduced from this experiment are somewhat different from those reported previously:

(i) Two mode couplings are actually observed.